JOURNAL OF MATERIALS SCIENCE 29 (1994) 5576–5582

Compatibility between PAN-based carbon fibres and Mg8Li alloy during the pressure infiltration process

S. KUDELA, V. GERGELY
Institute of Materials and Machine Mechanics, Slovak Academy of Sciences, POB 95, 830 08 Bratislava, Slovakia

E. JÄNSCH, A. HOFMANN
Institute of Materials Research, Technical University Chemnitz-Zwickau, POB 964, D-09009 Chemnitz, Germany

S. BAUNACK, S. OSWALD, K. WETZIG
Institute for Solid State and Materials Research, Institute for Solid State Analytics and Structural Research, POB 270016, D-01171 Dresden, Germany

The interaction of PAN-based T800H type carbon fibres, which had been coated with (i) pyrocarbon and (ii) pyrocarbon + SiC protective layers, was studied by means of SEM, energy-dispersive X-ray analysis and Auger electron spectroscopy. The interaction occurred during the pressure infiltration process at temperatures from 898 to 908 K and at contact times of 4–30 s. As detected by AES measurements, both Mg and Li penetrated throughout the carbon fibres, and Li_2C_2 was formed without remarkable reaction zone occurrence, which led to carbon fibre degradation. The pyrocarbon layer (about 50 nm thick) demonstrated a good protective efficiency and the corresponding metal-matrix composite exhibited satisfying strength characteristics; nevertheless, the influence of processing variables (temperature, time) was obvious. On the other hand, the double-coated pyrocarbon + SiC carbon fibres were strongly affected by Li_2C_2 formation.

1. Introduction

Magnesium–lithium alloys are known as the lightest metallic structural materials (1.4–1.6 g cm^{-3}) and by their reinforcement with high-strength fibres, metal-matrix composites (MMCs) with very high strength-to-weight ratio may be obtained. The pressure infiltration technology can be considered to be a suitable method for preparing MMCs with an MgLi matrix; nevertheless, the compatibility of reinforcements with molten MgLi alloys represents a serious problem because of the very high diffusional mobility and reactivity of Li. Some transition metals (Fe, Ti) are stable in contact with molten MgLi alloys, which facilitates the reinforcement of MgLi matrix with high-carbon steel and/or titanium alloy wires, leading to MMCs with excellent creep and strength characteristics [1, 2]. Their densities, however, are much higher than that of the MgLi matrix.

Carbon fibres (CFs) possess a low density and a high strength and therefore seem to be the most appropriate reinforcement, maintaining the low density of MMCs with an MgLi matrix. The system Mg–Li–C, however, is thermodynamically unstable and all efforts to manufacture MMCs of such a type have so far failed. As reported by Mason *et al.* [3], a lithium carbide Li_2C_2 was formed under squeeze infiltration conditions, leading to severe damage of CFs.

To achieve an effective protection of CFs against molten MgLi alloy attack it is necessary to coat them with stable protective layers. The aim of the present paper is to investigate the compatibility of PAN-based carbon fibres T800H (high-strength type) with molten Mg–8 wt%Li (Mg8Li) alloy during the pressure infiltration process after the fibres have been coated with (i) a pyrocarbon layer and (ii) a pyrocarbon + SiC double layer by chemical vapour deposition (CVD). We have studied the chemical and morphological changes of CFs caused by interaction with molten Mg8Li alloy by combining Auger electron spectroscopy (AES), energy-dispersive X-ray spectroscopy (EDX) and SEM in relation to the strength characteristics of prepared MMCs.

It was believed that a pyrocarbon (pyroC) coating should act as an effective barrier against lithium penetration due to the impermeability of benzene layers for Li atoms [4] as discussed in Section 4. The outer SiC layer was intended to promote the wetting of CF with molten Mg8Li alloy [5].

2. Experimental procedure

Continuous PAN-based carbon fibres T800H (Torray Industries Inc.) were used as the starting materials. Their basic characteristics were: tensile strength R_m

0022–2461 © *1994 Chapman & Hall*

= 5490 MPa, Young's modulus $E = 294$ GPa, elongation $A = 1.9\%$, density $\rho = 1.81$ g cm^{-3} [6]. After the fibres had been thermally desized, a pyroC layer about 50 nm thick was deposited by CVD from a $C_6H_6 + Ar$ vapour mixture at 1020–1320 K. The CF (pyroC) rovings, consisting of up to 6000 monofilaments, were then compacted with a silica binder (~5–7 wt %) to obtain a preform with about 50 vol % of CF. The double-coated pyroC + SiC carbon fibres were fabricated by CVD from a $CH_3SiCl_3 + H_2$ vapour mixture at 1320 K on the CF(pyroC) fibre surfaces so that the outer SiC layer was about 100 nm thick, and then they were compacted with silica binder to obtain a preform with about 27 vol % of fibres. The procedures used for CVD coating of CFs are described in detail by Plänitz *et al.* [7].

The Mg–8 wt % Li alloy for infiltration experiments was prepared using both Mg (purity 99.9%) and Li (purity 99.5%) as starting raw materials by casting under argon pressure (1 MPa) in a steel crucible. The alloy consisted of a two-phase h.c.p.–b.c.c. structure in the solid state, with a liquidus temperature of 860 K.

Both CF (pyroC) and CF(pyroC + SiC) preforms (37 mm × 10 mm × 3 mm) were infiltrated in a laboratory autoclave by submersion in the molten Mg8Li alloy (temperature T_i) under a vacuum $p_v \simeq 10$ Pa and following the action of argon pressure. Before the infiltration took place the preform had been preheated to $T_p \simeq 470$ K. The argon pressure was increased continuously with time t from the vacuum p_v up to the value of p_i. The infiltration time $t = t_2 - t_1$ is the interval between the start of argon inflow (t_1) and the infiltrated preform withdrawal (t_2). The diagram of temperature and pressure operations during the infiltration cycle is shown in Fig. 1.

3. Results

3.1. Microstructure and fractography

The fibre volume fractions V_f and in some cases also the pore volume fractions V_p of the MMC samples studied were evaluated by standard quantitative metallography procedures. The results obtained are presented in Table I, showing V_f variations within quite large concentration intervals. As seen, the pore fractions V_p tend to decrease with increasing infiltration pressure and duration of infiltration.

A typical polished cross-section of as-prepared CF(pyroC)–Mg8Li MMC is shown in Fig. 2, demonstrating that the CF bundle is well infiltrated with Mg8Li alloy. The SEM micrograph of Fig. 3 shows the detail of a deep-etched cross-section and indicates neither fibre–matrix interaction nor fibre damage. The fractographs of CF(pyroC)–Mg8Li tensile samples in Fig. 4a suggest maintenance of the original granular texture of CFs which, however, disappears progressively with increasing infiltration parameters.

Quite a different image is exhibited by the double-coated CF(pyroC + SiC) fibres in Mg8Li matrix. As

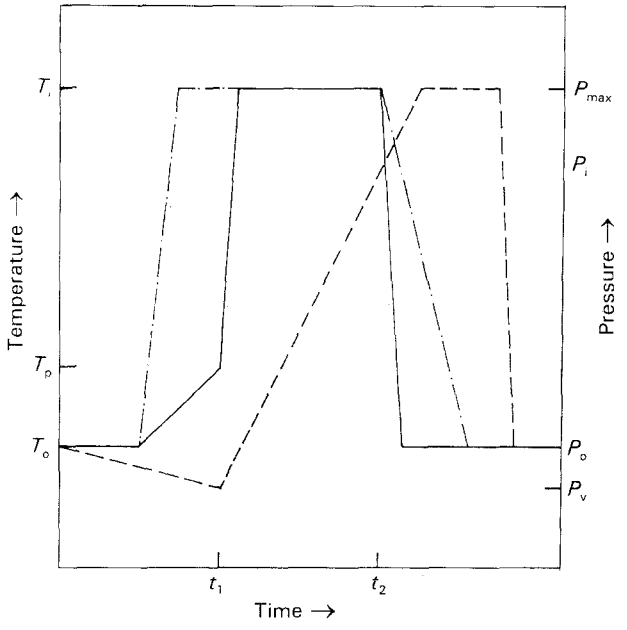

Figure 1 Diagram of the temperature and pressure operations during an infiltration cycle: (—) sample temperature, (— · —) liquid metal temperature, (— — —) gas pressure.

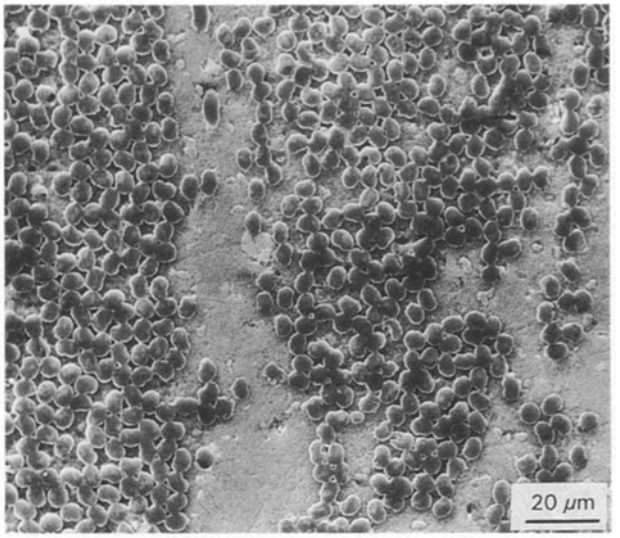

Figure 2 SEM micrograph of a polished section of CF(pyroC)–Mg8Li composite material.

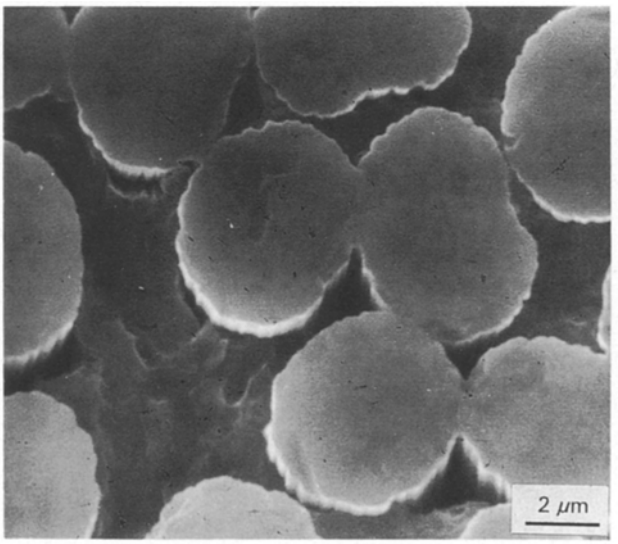

Figure 3 SEM micrograph of CF(pyroC) in an Mg8Li matrix. Deep-etched with 10% CH_3COOH solution in isopropanol.

TABLE I Results of infiltration experiments with coated carbon fibres: the infiltration variables are infiltration temperature T_i, time t and infiltration pressure p_i. The composite samples are characterized by the fibre volume fraction V_f, Young's modulus E, tensile strength R, normalized tensile strength R_n, reinforcement efficiency ζ_R and pore fraction V_p

Fibre coating	Infiltration variables			V_f	E	R	R_n	ζ_R	V_p
	T_i(K)	t(s)	p_i(MPa)	(%)	(GPa)	(MPa)	(MPa)		(%)
PyroC	900	4	0.9	0.45	76	680	744	0.58	0.067
	898	10	2.7	0.57	105	425	385	0.30	–
	899	15	3.8	0.40	86	345	406	0.32	0.042
	900	30	5.0	0.65	104	485	396	0.31	0.007
PyroC	909	4	0.9	0.54	92	480	452	0.35	0.067
	910	10	2.8	0.72	–	405	312	0.24	–
	907	15	3.8	0.69	94	–	–	–	–
	909	30	4.9	0.55	91	395	368	0.29	–
PyroC + SiC	900	4	0.9	0.33	65	156	185	0.22	–
	898	15	2.7	0.31	66	148	177	0.21	–
	898	30	3.8	0.21	59	121	150	0.17	–
PyroC + SiC	908	4	1.0	0.31	78	160	197	0.23	–
	907	15	2.8	0.24	60	89	77	0.09	–
	906	30	3.8	0.29	59	150	186	0.22	–

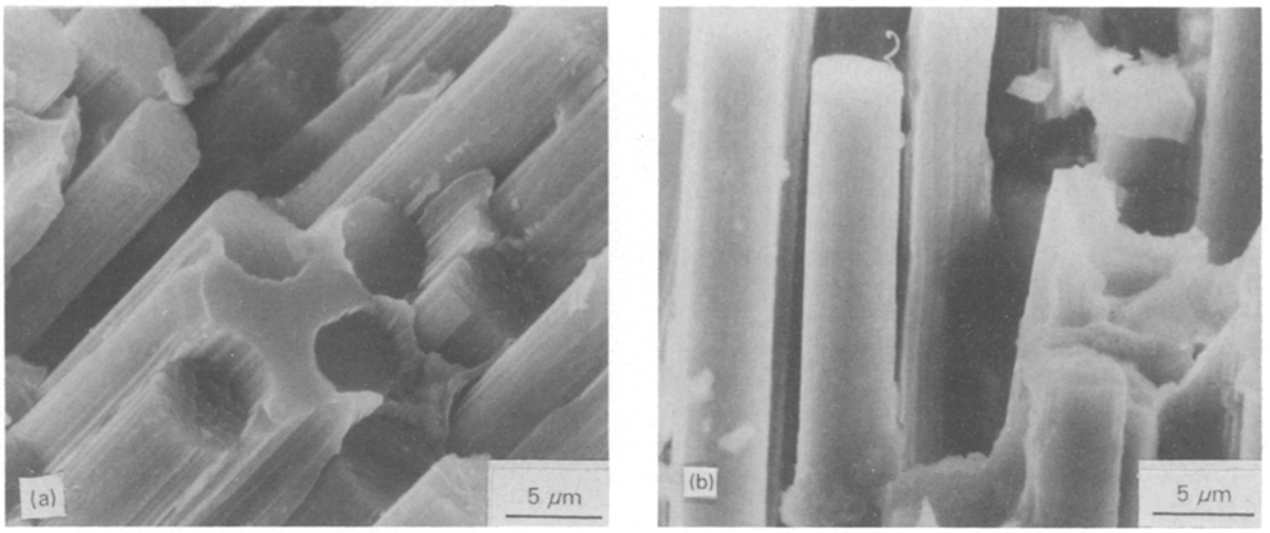

Figure 4 SEM micrograph of the fracture surface of CF(pyroC)–Mg8Li composite material after tensile tests: (a) prepared at 898 K/4 s, (b) prepared at 908 K/30 s.

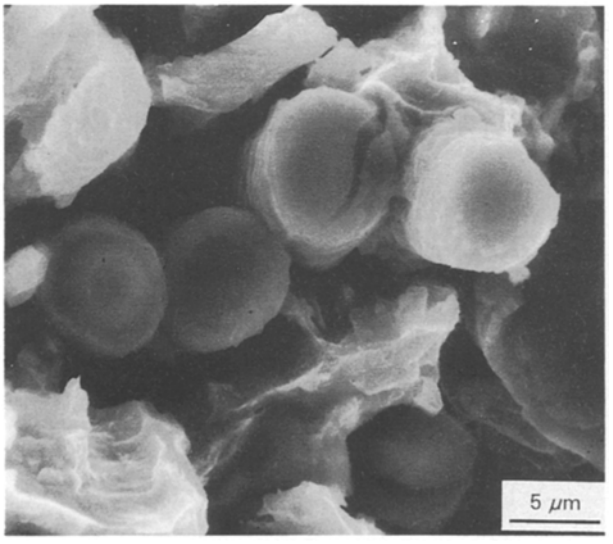

Figure 5 Fracture surface (SEM) of CF(pyroC + SiC)–Mg8Li composite material after a tensile test (898 K/30 s).

seen in Fig. 5, the (pyroC + SiC)-coated CFs were strongly attacked by molten Mg8Li alloy. The CFs exhibited flat fracture surfaces and the destruction of MMC samples in tensile tests occurred without pull-out, in contrast to the CF(pyroC)–Mg8Li MMCs where extensive pull-out took place during tensile deformation (Fig. 4b).

3.2. EDX and AES

Both EDX and AES investigations were carried out on mechanically polished sections of as-prepared MMC samples containing T800H carbon fibres with pyroC and/or pyroC + Si coatings. The polishing operations were accomplished using isopropyl alcohol (p.a. quality) as a waterless liquid medium.

The EDX analysis showed that cross-sections of CFs with pyroC + SiC double coating exhibited a markedly higher oxygen content than the surrounding Mg8Li matrix (Fig. 6a), whereas a similar effect was

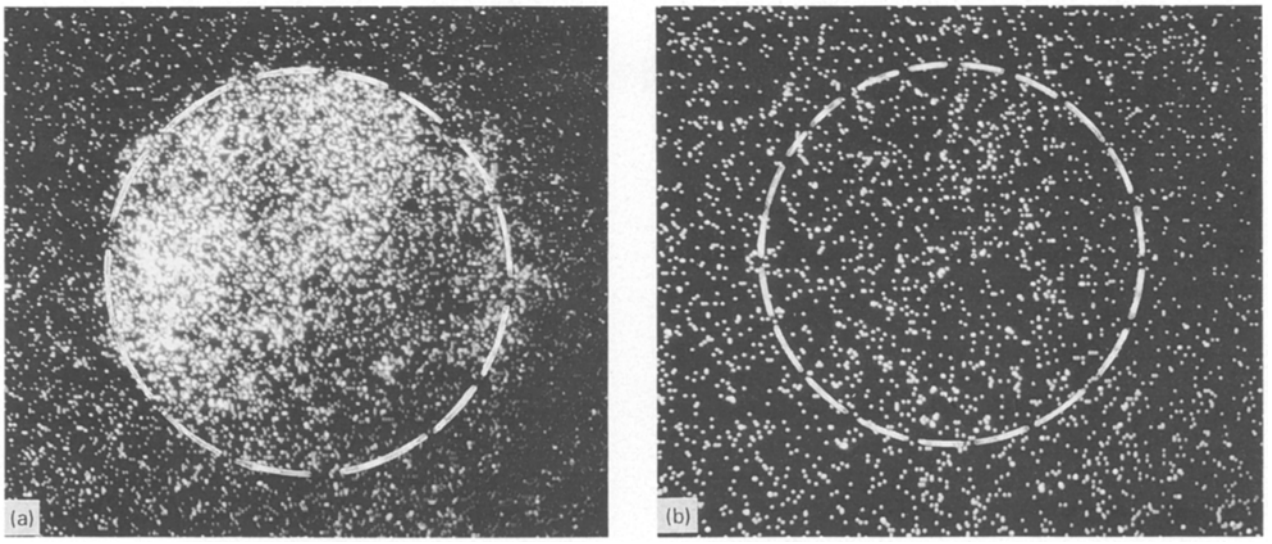

Figure 6 Oxygen distributions (OK_α) in carbon fibre cross-sections, marked by dashed circles: (a) CF(pyroC + SiC)–Mg8Li composite, (b) CF(pyroC)–Mg8Li composite.

observed to a substantially lesser degree or not at all in CFs coated with a single pyroC layer (Fig. 6b). No remarkable diffusion gradient of oxygen OK_α signals was demonstrated along CF cross-sections. To explain this phenomenon, AES with sputter depth profiling (Ar^+ ions, 3 keV, 200 nA cm^{-2}) were applied. The AES investigations were carried out in a VG Escalab Mk 4 (vacuum 5×10^{-8} Pa, lateral resolution less than 1 μm). AES line shapes taken from point measurements on a cross-section of pyroC + SiC double-coated CF in Mg8Li matrix are presented in Fig. 7a–e.

The AE lines in Fig. 7a and b represent extreme cases of observed C(KVV) spectral fine structure, whereby the peaks between 246 and 262 eV indicate carbide compound occurrence. The 30–46 eV AE peaks (Fig. 7c) were identified as arising from an Mg(LVV) transition, whereas those in Fig. 7d in an energy window of 41–54 eV correspond to the Li(KVV) transition, when a peak at 48–54 eV is significant. The identification of Mg(LVV) and Li(KVV) Auger transitions was performed using the AE spectra taken from pure Mg and Li metals as standards. The high-energy Mg(KLL) signal (1160–1180 eV) is very weak, almost at the background level (Fig. 7e).

Fig. 8 represents the intensity depth profiles of the AE spectral signals characterized above after sequential sputtering, where the maximum sputtering time of 69 min corresponds to a depth of about 400 nm. It is seen that on the CF cross-section surface a thin layer of oxidic compound about 20–30 nm thick is formed where, most likely, the oxygen is bonded with lithium (f and c lines), and below this layer the carbide compound is situated together with elemental Mg and Li. Li_2C_2 is the only carbide compound coming into consideration here, as the formation of magnesium carbides MgC_2 and Mg_2C_3 by direct synthesis is thermodynamically unfavourable [8]. The occurrence of elemental Li can be caused by electron-beam decomposition of the corresponding compounds. It is believed that on the contact of CFs containing Li_2C_2

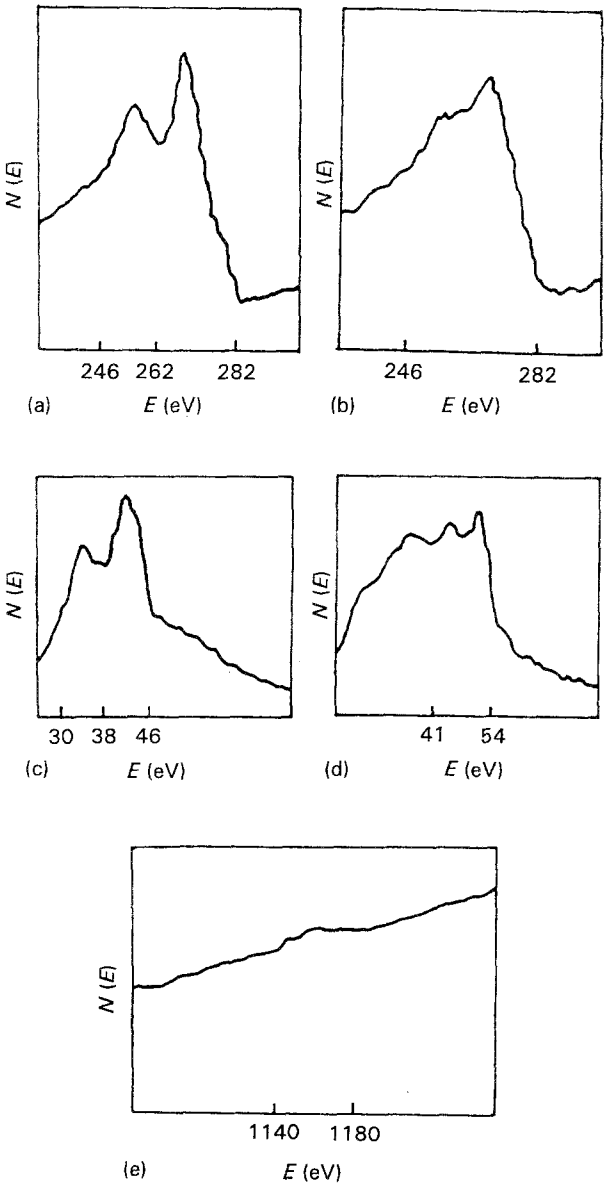

Figure 7 AES line shapes taken from carbon fibre sections in CF(pyroC + SiC) composite material: (a,b) C(KVV) (246–282 eV), indicating carbide compound occurrence; (c) Mg(LVV) (30–46 eV), (d) Li(KVV) (41–54 eV), (e) Mg(KLL) (1160–1180 eV).

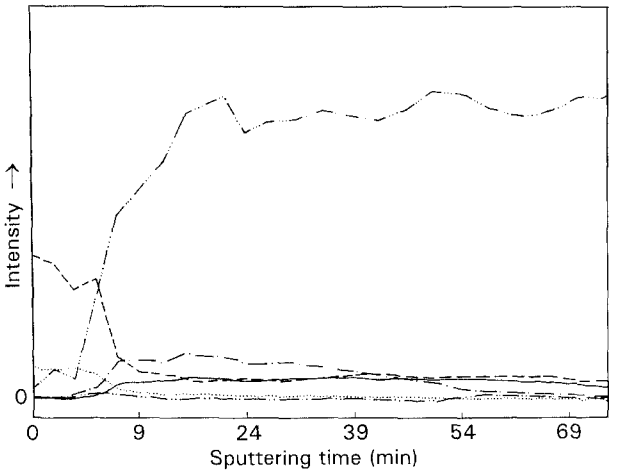

Figure 8 Intensity depth profiles of Auger spectra depicted in Fig. 7 together with O(*KVV*): (— · —) Fig. 7a, (— · · · —) Fig. 7b, (· · ·) Fig. 7c, (—) Fig. 7d, (— · · —) Fig. 7e, (— —) O(*KVV*).

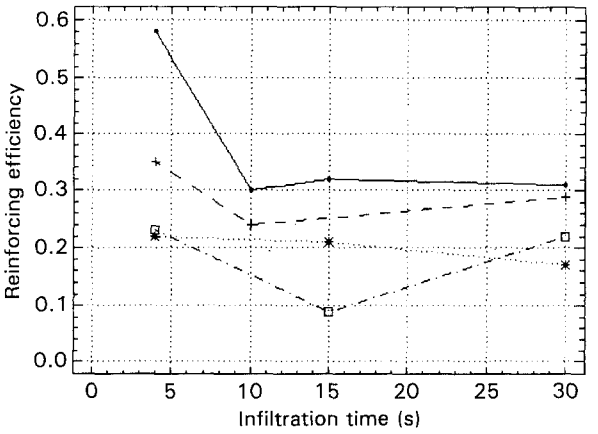

Figure 9 Reinforcing efficiency versus pressure infiltration process variables (time, temperature) of CF(pyroC) and CF(pyroC + SiC) reinforced Mg8Li matrix composites: (■, —) 898 K, pyroC; (+ , — —) 908 K, pyroC; (∗, · · ·) 898 K pyroC + SiC; (□, — · —) 908 K, pyroC + SiC.

with air moisture a LiOH layer is formed by the reaction

$$Li_2C_2 + 2H_2O = 2LiOH + C_2H_2 \quad (1)$$

which explains the oxygen gettering effect observed by EDX analysis on the CF cross-sections. Thus, the oxygen distribution OK_α maps the occurrence of Li_2C_2 on CF cross-sections; nevertheless, lateral growth of the LiOH layer must also be taken into account.

3.3. Mechanical properties

Samples of both as-cast C(pC)–Mg8Li and C(pC + SiC)–Mg8Li types of MMC, which had been prepared by the pressure infiltration route, were used to measure the tensile strength R and Young's modulus E. The reinforcing efficiency ζ_R was defined by the formula

$$\zeta_R = R_n/R_c \quad (2)$$

where R_n is the tensile strength of MMC normalized to a fibre concentration of $V_f = 0.5$, and R_c is the tensile strength of the corresponding MMC calculated by means of the rule of mixtures:

$$R_c = R_f V_f + R_m V_m \quad (3)$$

where R_f and R_m are the stresses in fibre yarns and in the matrix, respectively, and $V_f = V_m = 0.5$ are the fibre and matrix normalized concentrations. The tensile strength of the Mg8Li matrix $R_m = 100$ MPa was experimentally determined, whereas R_f was calculated using the two-parameter Weibull distribution [9]:

$$R_f = R_o(L_o)\ m^{-1/m}\exp(-1/m) \quad (4)$$

where $R_o(L_o)$ is the scale parameter at the fibre test length L_o and m is the Weibull modulus. The $R_o(L_o)$ and m values of starting CF(pyroC) as well as CF(pyroC + SiC) rowings were evaluated for $L_o = 12$ mm and the results obtained were as follows:

$$CF(pyroC): R_o(L_o) = 4002\ MPa \quad m = 5.6$$

$$CF(pyroC + SiC): R_o(L_o) = 2897\ MPa \quad m = 4.2$$

The R_f values calculated using Equation 4 were then

$$CF(pyroC): R_f = 2461\ MPa$$

$$CF(pyroC + SiC): R_f = 1622\ MPa$$

and finally from Equation 3 the normalized R_c values were obtained. The tensile strength R of as-prepared MMCs was determined by a standard tensile test using an Instron-type machine (crosshead speed of 0.1 mm min^{-1}) whereas the E modulus was evaluated by a four-point bend test.

R, R_n, ζ_R as well as E values of the corresponding MMCs are summarized in Table I together with infiltration process variables and some structural characteristics (fibre concentration, porosity) of the corresponding as-cast MMCs. It is seen that CF(pyroC)–Mg8Li MMCs displays a considerably higher tensile strength R than those reinforced with double-coated pyroC + SiC carbon fibres. This can be attributed to the substantially different CF concentrations as well as some fibre degradation due to the outer SiC layer deposition; nevertheless, a significant difference in the reinforcing efficiency ζ_R between CF(pyroC) and CF(pyroC + SiC) reinforcements is also obvious, especially in cases of short infiltration times (Fig. 9). The E-modulus values were less sensitive to the infiltration process variables. For comparison, the E-modulus of Mg8Li alloy is 42 GPa.

4. Discussion

Lithium, like other alkali metals, readily enters the graphite lattice at elevated temperatures and after losing its electron it migrates as an Li^+ ion through the host lattice by thermally activated hops. The most favourable diffusion routes are the directions parallel to the basal hexagonal planes, while Li^+ movement across the basal planes is exceedingly disadvantageous from the energy point of view. Using an *ab initio* procedure, Boehm and Banerjee [4] have estimated the energy barrier for passage of Li^+ across the hexagonal plane to be ~ 15 eV, whereas for in-plane movement the energy barrier is reported to be only ~ 0.7 eV. Experiments performed by Jungblut and

Hoinkis [10] with highly oriented pyrographite have also confirmed that the probability of an Li^+ ion crossing the basal planes is negligible. These results suggest that Li^+ migration in carbon materials is strongly interplanar, and as such it should be critically influenced by the basal plane texture.

The pyroC layer as deposited from hydrocarbon precursors at moderate temperatures (below 1600 K) consists of benzene-type hexagons forming planar blocks oriented mainly parallel to the substrate, exhibiting some distortion between adjacent elementary layers. Starting from the concept of Maire and Mering [11], the pyroC layer can be presented as a combination of hexagonally bonded carbon atoms (sp^2 states) and "unorganized" interstitial carbon atoms which are strongly bonded to the elementary layers, increasing their separation (sp^3 states). The sp^2 and sp^3 states can be well identified by Raman spectroscopy, where the Raman bands at 1575 cm^{-1} (G-lines) correspond to sp^2 states while those at 1354 cm^{-1} (D-lines) come from sp^3 states, and the ratio of intensities I(G) to I(D) is a measure of the size of graphite crystallites (planes) aligned in the direction of the fibre surface [12]. PyroC-coated CFs similar to those used in our experiments were investigated by the above-mentioned method by Than *et al.* [13], who concluded that the I(G) to I(D) ratio was about 2:1 for the pyroC layer and about 1:1 for basic PAN-based CFs, respectively (Fig. 10). Thus, a relatively well organized sheet texture of aromatic layers is expected to form by the CVD process from benzene precursors on the CF surface, which due to the clearly interplanar character of Li^+ diffusion can impede Li penetration into the CF interior. This aspect can explain the rather high stability of pyroC-coated T800H carbon fibres in contact with molten Mg8Li alloy during infiltration experiments.

The pyroC coating on CFs was designed to provide a diffusion barrier against Li penetration. Nevertheless, as manifested by extensive pull-out such coatings have demonstrated a poor wettability by the Mg8Li matrix. The deposition of an outer SiC coating rather enhanced the wettability of CF; however, the protective efficiency of the double pyroC + SiC coating was lowered because of the instability of the outer SiC layer in contact with molten Mg8Li alloy, as well as by damage of the inner pyroC layer by SiC deposition. SiC decomposition can occur most probably by the reaction

$$4Mg + 2Li + 2SiC = 2Mg_2Si + Li_2C_2 \qquad (5)$$

The absence of accurate thermodynamic data makes it impossible to calculate the exact free enthalpy changes of this reaction. Mason *et al.* [3] have estimated $\Delta G^\circ_{600\,K} = -(18 \pm 25)\ kJ\ mol^{-1}$, i.e. it is difficult to decide explicitly on the feasibility of SiC decomposition by Reaction 5; nevertheless, its thermodynamic potential seems to be low.

The occurrence of defects in pyroC + SiC layers can radically decrease their chemical resistance against molten MgLi alloy attack. As the CVD process was carried out at rather low temperatures (1320 K), SiC + Si codeposition [14, 15] as well as SiC lattice distortion [15] could take place. Free silicon is readily soluble in a molten MgLi matrix, precipitating as Mg_2Si primary crystals [16]. Although we have found Mg_2Si crystals in the Mg8Li matrix, their formation by interaction of silica binder with Mg8Li alloy must also be taken into account. A small amount of silicon was also detected by EDX and AES in (pyroC + SiC)-coated CF cross-sections. It is believed that double pyroC + SiC coating failure can be attributed mainly to the presence of silicon in the pyroC layer (perhaps as badly crystallized SiC clusters), which can react with molten MgLi alloy according to Reaction 5 after the outer SiC layer has failed due to the dissolution of free silicon.

Li penetration into carbon materials is accompanied by the formation of intercalating compounds $LiC_n (n \geqslant 6)$ and/or the ionic carbide compound Li_2C_2. According to Guerard and Herold [17] the intercalation of carbon materials (including carbon fibres) starts at ~670 K and, however, at ~720 K this accelerates the formation of lithium carbide Li_2C_2 which seems to be promoted by the presence of foreign atoms. Asano *et al.* [18] have measured a dissociation pressure p_{Li} over Li_2C_2 at temperatures of 614–725 K, and an extrapolation of $p_{Li}(T)$ dependence towards higher temperatures suggests that decomposition of Li_2C_2 occurs at ~900 K. The $p_{Li}(T)$ dependence presented by Katskov *et al.* [19] implies that thermal decomposition of Li_2C_2 begins at ~960 K.

The chemical changes of CF taking place in the infiltration process were detected by changes in C(KVV) Auger line shape, suggesting lithium carbide Li_2C_2 formation as the magnesium carbides MgC_2 and Mg_2C_3 could not be formed by direct synthesis. No significant reaction zone has been observed; thus it is believed that Li_2C_2 formation occurs after the Li has penetrated throughout the fibre volume. As shown in Fig. 9, progress of the interaction of CF with an

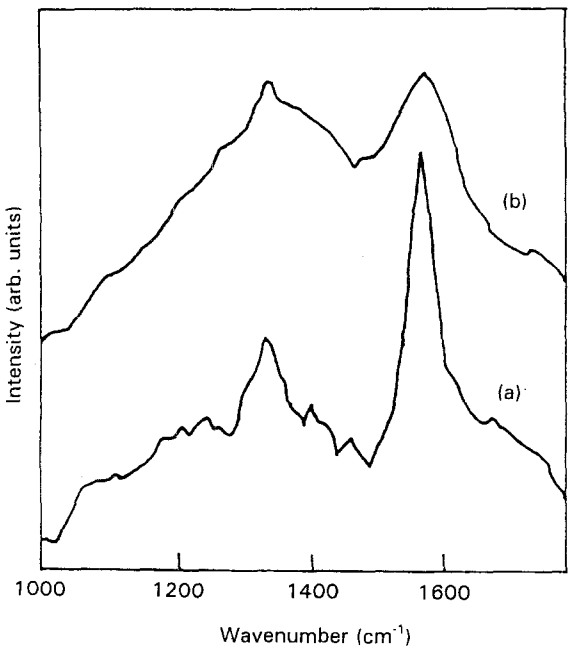

Figure 10 Raman spectra taken from PAN-based carbon fibres (a) coated with pyroC, (b) uncoated, according to Than *et al.* [13].

Mg8Li matrix is accompanied by a drop in the strengthening efficiency, whereby a dependence on both process variables (temperature, time) as well as different protective coatings is evident. Morphological changes also occurred in CF and were characterized by the gradual disappearance of a rough granular texture. Thus, the degradation process in CFs can be attributed to damage of the basal aromatic plane chains oriented parallel to the fibre axis by the formation of ionic lithium carbide Li_2C_2 (crystal lattice of BaC_2 type), i.e. a total rearrangement of carbon atoms takes place here.

As shown by AES, lithium and magnesium penetrated in parallel to the CF interior. Although the formation of carbide compound containing Mg is not expected, the results presented by Viala *et al.* [20] suggest that some chemical and microstructural modifications of CFs due to Mg treatment decreasing their mechanical properties cannot be excluded.

5. Conclusions

The interaction of molten Mg–8 wt% Li alloy with PAN-based carbon fibres T800H, coated with (i) pyrocarbon and (ii) pyrocarbon + SiC, has been studied. The interaction took place during the infiltration process at temperatures of 898 and 908 K and contact times of 4–30 s, under argon pressure. The following results were obtained.

1. Carbon fibres coated with a pyrocarbon layer manifested a much higher morphological stability in contact with molten Mg8Li alloy than those coated with a double pyrocarbon + SiC layer under the same infiltration conditions. The latter were strongly damaged during the infiltration process.

2. AES measurements have shown that both Mg and Li penetrated throughout the carbon fibres. Lithium carbide Li_2C_2 formation was indicated by changes of shape of C(*KVV*) Auger lines. The degradation of carbon fibres was attributed to this Li_2C_2 formation.

3. An extensive pull-out effect indicates that the pyrocarbon-coated carbon fibres are poorly wetted with molten Mg8Li alloy; nevertheless, their reinforcing efficiency calculated from tensile strength values is markedly higher than that determined for pyrocarbon-coated carbon fibres, where the influence of infiltration process variables (temperature, time) was significant.

References

1. B. A. WILCOX and A. H. CLAUER, *Trans. Met. Soc. AIME* **245** (1969) 935.
2. V. S. IVANOVA, I. M. KOPYEV, F. M. YELKHIN and Yu. E. BUSALOV, "Alyuminievye i magniyevye splavy armirovanye voloknami" (Nauka, Moscow, 1974) p. 199.
3. J. F. MASON, C. M. WARWICK, P. J. SMITH, J. A. CHARLES and T. W. CLYNE, *J. Mater. Sci.* **24** (1989) 3934.
4. R. C. BOEHM and A. BANERJEE, *J. Chem. Phys.* **96** (1992) 1150.
5. T. WADA, G. T. ELDIS and D. L. ALBRIGHT, US Patent 4 657 065, (1987).
6. Torayca Data Sheet (Toray Deutschland GmBH, 1991).
7. H. PLÄNITZ, G. BOCHMANN, W. WAGNER, M. SEIDLER and E. WOLF, *Wiss. Z. TU Chemnitz* **32** (1990) 218.
8. JANAF Thermochemical Tables, 2nd Edn, Vol. 37 (US Department of Commerce NSRDS-NBS 1971).
9. B. D. COLEMAN, *J. Mech. Phys. Solids* **7** (1958) 60.
10. B. JUNGBLUT and E. HOINKIS, *Phys. Rev.* **B40** (1989) 10810.
11. J. MAIREE and J. MERING, "Graphitization of Soft Carbon" in "Chemistry and Physics of Carbon", edited by Dekker, NY, Walker, Vol. 6 (Ph. I. 1970) p. 125.
12. G. MARX, P. W. MARTIN, N. MEYER and K. NESTLER, *Fresenius J. Anal. Chem.* **346** (1993) 181.
13. W. THAN, A. HOFMANN and G. LEONHARDT, *ibid.* **346** (1993) 37.
14. Y-S. PARK, M-H. KIM and J-Y. LEE, *J. Mater. Sci. Lett.* **8** (1989) 321.
15. K. MINATO and K. FUKUDA, *J. Mater. Sci.* **23** (1988) 699.
16. K. SCHEMME, "Entwicklung superleichter Magnesiumwerkstoffe" (VDI Verlag GmbH, Düsseldorf, 1993).
17. D. GUERARD and A. HEROLD, *Carbon* **13** (1975) 337.
18. M. ASANO, K. KUBO and H. KIMURA, *J. Nucl. Mater.* **102** (1981) 353.
19. D. A. KATSKOV, B. V. LVOV and V. I. DANILKIN, *Zh. Prikl. Spektrosk.* **27** (1977) 685.
20. J. VIALA, P. FORTIER, G. CLAVEYROLAS, H. VINCENT and J. BOUIX, *J. Mater. Sci.* **26** (1991) 4977.

Received 16 December 1993
and accepted 22 April 1994